

Chapter 2

Thermodynamic Principles of Self-Healing Metallic Materials

In this chapter, the thermodynamics of self-healing is considered with an emphasis on metallic materials. All complex biological organisms have the ability to repair minor damage. Incorporating the self-repair function into inorganic systems is of growing interest for materials scientists. So far, most recent studies have concentrated on polymers and ceramics because it is easier to incorporate self-healing in nonmetallic materials than in metallic materials. However, metallic self-healing alloys and composites are of great practical importance. We review the design principles of self-healing materials using the nonequilibrium thermodynamics approach and the concept of hierarchical organization. The generalized thermodynamic force that leads to healing is induced by bringing the system away from thermodynamic equilibrium. We focus on the three major methods of imparting the ability for self-healing in metallic systems: precipitation-induced healing, embedding shape-memory alloys, and embedding a low-melting point alloy in the alloy matrix.

2.1 Introduction

Self-healing inorganic materials or material systems constitute a novel field of materials science that emerged relatively recently and started to rapidly expand (Files and Olson 1997; Feng et al. 2000; Zwaag 2007; Ghosh 2009). Self-healing in biological objects is a source of inspiration for this new research area. Most living tissues or organisms can heal themselves, provided the incurred damage is moderate. For example, after cutting, blood flows into the wound and clots, thus sealing the defect and allowing the skin to repair itself (Burgess 2002). A crack in bones is repaired due to regeneration of bone material. Most engineered materials; however, deteriorate with time irreversibly due to wear, brittle fracture, fatigue, creep, and other modes of degradation, which limits the life of various components and sometimes

causes catastrophic damage. It would be very desirable to implement the ability of self-healing in inorganic materials, so that when these materials are cracked or damaged, a healing agent could be triggered to flow into the damaged area to “heal” the damage, essentially sealing the cracks. Whereas the inorganic system would not be able to create identical new material to replace the damaged area, the self-repair function could serve to provide new material in the damaged area, similar to the way in which an injury to the skin results in the formation of a scar.

As engineering systems become more sophisticated and mimic more characteristics of biological systems (Zhou 2000; Bruck et al. 2002), many new beneficial concepts can be realized. It is emphasized that the biological mechanisms of healing are very complex and often involve many factors acting concurrently. There is a growing understanding by materials scientists who work on the development of self-healing materials that the biological mechanisms of healing cannot be directly borrowed for artificial materials. For instance, Van Der Zwaag (2009) note that “while Nature has shown an extreme diversity in microstructures and microstructural systems, and, subsequently, has shown a wide diversity of healing mechanisms, it is unwise to try to copy these healing mechanisms in man-made engineering materials in a direct manner. Engineering materials have their own characteristics, and, in designing self-healing behavior in such materials, their intrinsic or natural character has to be taken into account.” Therefore, we prefer to speak about bio-inspired, rather than biomimetic, self-healing materials.

To date self-healing has been applied most successfully in polymers, and this is because of their relatively large rates of diffusion due the presence of the cross-molecular bonds (Anderson et al. 2007; Bond et al. 2007; Zhang et al. 2009). One way to create self-healing polymers is to use thermosetting polymers that have the ability to cure (toughening or hardening by cross-linking of polymer chains), such as the thermosetting epoxy (White et al. 2001; Sarikaya and Aksay, 1995; Jones et al. 2007; Toohey et al. 2007). Epoxy is a polymer formed by a reaction of an epoxide resin with polyamine hardener. Epoxy can serve as a healing agent that is stored within thin-walled inert brittle macrocapsules embedded into the matrix along with a catalyst or hardener (also embedded in the matrix, but separate from the latter). When a crack propagates, the capsules fracture and the healing agent is released and propagates into the crack because of capillarity. Then the healing agent mixes with the catalyst embedded in the matrix, which triggers the cross-linking reaction and hardening of the epoxy that seals the crack (White et al. 2001; Trask and Bond 2006; Trask et al. 2007; Williams et al. 2007; Wool 2008). A different approach involves thermoplastic polymers, with various ways of incorporating the healing agent into the material. In this approach, heating is often required to initiate healing, since thermoplastics soften and flow with increasing temperature.

Besides the polymers, ceramic self-healing materials are being developed, with the main focus on concrete composites. For example, a concrete composite was produced with hollow glass fibers containing an air curing sealant embedded in the concrete matrix (Dry 1994; Li et al. 1998; Nakao et al. 2006). This composite exhibited the self-healing behavior but it suffered from a significant (10–40%) loss of stiffness compared with standard concrete due to the fibers. This is a typical

situation, when a compromise between self-healing and mechanical properties should be sought. In another project involving self-healing ceramics, researchers have studied the crack-healing behavior and mechanical properties of a mullite composite toughened by the inclusion of 15% (by volume) SiC whiskers (Nakao et al. 2006; Takahashi et al. 2007). Self-healing ceramic materials often use oxidative reactions, because the volume of oxide exceeds the volume of the original material, and therefore, products of these reactions, due to their higher volume, can be used to fill small cracks (Zwaag 2009). Self-healing nanocomposites constitute another area of research.

The field of self-healing metals and metal composites has received serious attention only in the last 10 years (Lumley 2007; Wang et al. 2007; Manuel 2009, 2007; Manuel et al. 2009). It is much more difficult to heal metallic materials than polymers, because metallic atoms are strongly bonded and have small volumes and low diffusion rates. Currently, there are three main directions which have been taken in the development of self-healing metallic systems. First is the formation of precipitates at the defect sites that immobilize further growth until failure. Van Der Zwaag (2009) and co-workers called this mechanism “damage prevention” because the idea is to prevent the formation of voids by the diffusion of the precipitate from an oversaturated solid–solid solution (alloy). The driving mechanism for the diffusion is the excess surface energy of the microscopic voids and cracks that serve as the nucleation centers of the precipitate that plays the role of the healing agent by filling up the voids. As a result, the newly formed void is sealed before it grows and thus minimizes the creep and fatigue.

Second, Olson (1997), Manuel (2007), and co-workers (Bender and Olson 2008) used another approach: reinforcement of an alloy matrix with microfibers or wires made of a shape-memory alloy (SMA), such as nitinol (NiTi). SMA wires have the ability to recover their original shape after some deformation has occurred if they are heated above a certain critical temperature (Wang et al. 2005; Olson and Hartman 1982; Olson et al. 2009). If the composite undergoes crack formation, heating the material will activate the shape recovery feature of the SMA wires which then shrink applying compressive force at the cracks and close the cracks.

The third approach is to use a healing agent (such as an alloy with a low-melting temperature) embedded into a metallic matrix, similarly to the way it is done with the polymers. However, encapsulation of a healing agent into a metallic material is much more difficult task than in the case of polymers. The healing agent should be encapsulated in microcapsules which serve as diffusion barriers and which fracture when a crack propagates.

Self-healing can be viewed as a self-organization process that leads to increasing orderliness of the material and thus, decreasing entropy. From the viewpoint of thermodynamics, self-healing is a nonequilibrium process. In most self-healing schemes, the self-healing material is driven away from the thermodynamic equilibrium either by the deterioration process itself or by an external intervention, such as heating. After that, the composite slowly restores thermodynamic equilibrium, and this process of equilibrium restoration drives the healing. In the following sections, we discuss the general principles of the nonequilibrium thermodynamics of

self-healing, and focus on how the self-healing function might be incorporated in metal matrices, and how various processing methods could be employed to do so, emphasizing the thermodynamic aspects of self-healing.

2.2 Thermodynamics of Self-Healing

Self-healing materials possess many features of self-organizing systems, which have been studied intensively by physicists and chemists during the past half-century (Prigogine 1961; Prigogine and Nicolis 1977), whereas net entropy grows with time in most conventional systems in accordance with the Second Law of thermodynamics. As irreversible energy dissipation occurs and deterioration accumulates, self-organizing systems may exhibit increasing orderliness and self-organization. They are thermodynamically open systems that operate far from thermodynamic equilibrium and can exchange energy, matter, and entropy with the environment.

2.2.1 Entropy of a Hierarchical System

Entropy is a measure of irreversibility and disorder. The classical thermodynamic definition of entropy, S , was introduced in 1850s by R. Clausius as

$$dS = dQ/T, \quad (2.1)$$

where T is temperature and Q is heat exchanged. Entropy is an additive function (the net entropy of a system is equal to the sum of entropies of its parts). When heat dQ is transferred from a body with temperature T_1 to a body with temperature T_2 , the net entropy changes for the amount $dS = -dQ/T_1 + dQ/T_2$. Thus, if heat is transferred from a hotter body to a colder one ($T_1 > T_2$), the net entropy grows ($dS > 0$). This provides a convenient formal basis for the Second Law of thermodynamics stating that the net entropy of a closed system either remains constant (for a reversible process) or grows (for an irreversible process).

In 1877, L. Boltzmann suggested a definition of entropy using the statistical thermodynamic approach and the concept of microstates

$$S = k \ln \Omega, \quad (2.2)$$

where k is Boltzmann's constant, and Ω is the number of microstates corresponding to a given macrostate. Microstates are arrangements of energy and matter in a system that are distinguishable at the atomic or molecular level, but are indistinguishable at the macroscopic level (Craig 1992). A system tends to evolve into a less-ordered

(more random) macrostate which has a greater number of corresponding microstates, and thus the “configurational” entropy given by (2.2) grows.

Processes that lead to degradation (wear, corrosion, fatigue, fracture, creep, etc.) often involve interactions with different characteristic length scales, so that different isolated hierarchical levels (macro-, micro-, and nanoscale) can be distinguished in the system in a natural way. For example, friction and wear involve the contact of micro-, macro-, and nanoscale asperities and wear particles, capillary interactions, adhesion, and chemical molecular bonding (Nosonovsky and Bhushan 2007a; 2008d). In most cases, these interactions lead to irreversible energy dissipation and, therefore, to the production of entropy. However, in certain cases the entropy production at a particular scale level may be compensated by the entropy consumption at another level. Since the processes at different scale levels are independent and entropy is an additive function, the net entropy can be presented as the sum of entropies associated with the structures and process at corresponding scale levels

$$\Delta S_{\text{net}} = \Delta S_{\text{macro}} + \Delta S_{\text{micro}} + \Delta S_{\text{nano}}, \quad (2.3)$$

where the indices “net,” “macro,” “micro,” and “nano” correspond to the net entropy, macroscale, microscale, and nanoscale components (Nosonovsky and Esche 2008a, b; Nosonovsky 2009, 2010a, b).

As an example, let us consider a solid homogeneous body. The micro/nanoscale level corresponds to the vibrations of atoms in the crystalline lattice and is not of interest for us at this point. The mesoscale structures, such as grains, defects, and dislocations correspond to the microscale levels. A perfect single-crystal body with no defects has lower microscale entropy ΔS_{micro} than a body with such defects. Larger scale defects such as cracks and voids contribute to the macroscale component of the entropy, ΔS_{macro} . A material or a surface with a regular microstructure (e.g., a microtextured surface) is more ordered and thus it has lower microscale configurational entropy, ΔS_{micro} than a material with an irregular microstructure or surface texture (Nosonovsky and Esche 2008b).

This can be utilized for the healing of macroscale defects. Suppose there is excess entropy, ΔS_{macro} , associated with the macroscale defects, such as cracks or voids. Healing can be triggered by affecting the mesoscale structure, e.g., by the release of microcapsules. The fracture of the microcapsules decreases the orderliness of the microstructure and thus increases the entropy for ΔS_{micro} . In the case $|\Delta S_{\text{macro}}| < -\Delta S_{\text{micro}}$, the healing is done by decreasing the macroscale component of entropy at the expense of the mesoscale component (Nosonovsky et al. 2009). In other words, for most practical applications, the macroscale integrity and orderliness of material are of interest, and thus the expression for net entropy given by (2.3) can be truncated at the macroscale level, $\Delta S_{\text{net}} = \Delta S_{\text{macro}}$. The orderliness of the material, as observed at the macroscale, can grow (and, therefore, entropy can decrease) at the expense of excess entropy production at the lower scales. This is analogous to the crystal grain growth (e.g., in aluminum) due to thermal fluctuations; with growing grains, material structure becomes more ordered,

however, dissipation and excess entropy production occur at the nanoscale every time a grain border propagates (Nosonovsky and Esche 2008b).

2.2.2 *Thermodynamic Forces that Drive Healing*

In nonequilibrium thermodynamics, a thermodynamic force Y_i and a thermodynamic flow $J_i = \dot{q}_i$ are associated with every generalized coordinate q_i . In the widely accepted linear approximation, the flows are related to the forces by

$$J_k = \sum_i L_{ki} Y_i, \quad (2.4)$$

where L_{ki} are Onsager coefficients (De Groot and Mazur 1962). The heat production per unit time is given by

$$\frac{dQ}{dt} = \sum_i J_i Y_i, \quad (2.5)$$

and the rate of entropy production is

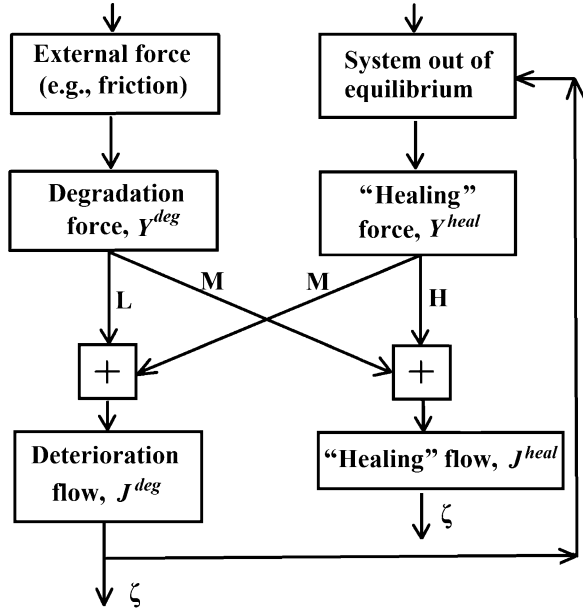
$$S = \frac{dQ}{T dt} = \frac{1}{T} \sum_i J_i Y_i, \quad (2.6)$$

a linear function of thermodynamic flows.

In order to characterize degradation, it is convenient to introduce a so-called “degradation parameter” ξ , to represent, for example, the wear volume or the total area of the cracks. The degradation parameter is a generalized coordinate of the degradation process. Note that the dimension of ξ can be different depending on the physical meaning of the degradation parameter. Thus, it may have the dimension of volume or area. The corresponding thermodynamic flow (or the rate of degradation) is linearly related to the thermodynamic forces (2.4) and entropy rates (2.6). The physical meaning of this proportionality is that a constant fraction of the dissipated energy is spent for the deterioration in a given process and under given operating conditions. The dimensions of the flow and generalized force are dependent on the dimension of the degradation parameter. It is easy to generalize for the case of several degradation parameters that correspond to several processes; however, we concentrate on the case of a single degradation parameter.

When a self-healing mechanism is embedded in the system, another generalized coordinate, the healing parameter, ζ , can be introduced, for example, the volume of released healing agent. Again, the corresponding thermodynamic flow is linearly related to the thermodynamic forces (2.4) and entropy rates (2.6). However, the degradation and healing processes usually have characteristic scale lengths and thus

Fig. 2.1 Block diagram of the healing process. Deterioration (or degradation) is caused by an external force. The deteriorated system is brought out of equilibrium so that the restoring (“healing”) force is created, which is coupled with the degradation flow through the parameter M



belong to different hierarchy levels, as was discussed above. The generalized degradation and healing forces are external forces that are applied to the system, and flows are related to the forces by the governing equations

$$\begin{aligned} J^{deg} &= LY^{deg} + MY^{heal}, \\ J^{heal} &= NY^{deg} + HY^{heal}, \end{aligned} \quad (2.7)$$

where L, M, N, H are corresponding Onsager coefficients (Fig. 2.1). It is expected that $L > 0, H > 0$ (degradation and healing grow when corresponding positive forces are applied), $M < 0, N < 0$ (degradation and healing decrease when opposite forces are applied), and $N = M$ due to the Onsager reciprocity condition (De Groot and Mazur 1962).

The degradation force Y^{deg} in (2.7) is an externally applied thermodynamic force that results in the degradation. The healing force Y^{heal} is an external thermodynamic force that is applied to the system. In most self-healing mechanisms, the system is placed out of equilibrium and the restoring force emerges, so we can identify this restoring force with Y^{heal} . Since the restoring force is coupled with the degradation parameter ζ by the negative coefficients $N = M$, it also causes a degradation decrease or healing.

The entropy rate is given, using (2.6) and (2.7), by

$$\dot{S} = \dot{S}^{deg} + \dot{S}^{heal} = \frac{L}{T}(Y^{deg})^2 + \frac{2M}{T}Y^{deg}Y^{heal} + \frac{H}{T}(Y^{heal})^2. \quad (2.8)$$

The first term in the right-hand part of (2.8) corresponds to the degradation, $\dot{S}^{\text{deg}} = L(Y^{\text{deg}})^2/T$, while the healing term involves positive and negative parts $\dot{S}^{\text{heal}} = 2MY^{\text{deg}}Y^{\text{heal}}/T + H(Y^{\text{heal}})^2/T$. Assuming the scheme described by (2.3), when macroscale healing occurs at the expense of microscale deterioration, we postulate

$$\begin{aligned}\dot{S}_{\text{macro}} &= \frac{2M}{T} Y^{\text{deg}} Y^{\text{heal}}, \\ \dot{S}_{\text{micro}} &= \frac{H}{T} (Y^{\text{heal}})^2.\end{aligned}\tag{2.9}$$

The (2.7)–(2.9) can be easily generalized for the case of several degradation and healing parameters.

2.2.3 Friction-Induced Degradation

Surface is the most vulnerable part of a material sample, and not surprisingly, deterioration often occurs at the surface (wear, fretting, etc.) and is induced by friction. The empirical Coulomb (or Amontons–Coulomb) law of friction states that the dry friction force F is linearly proportional to the normal load force W

$$F = \mu W,\tag{2.10}$$

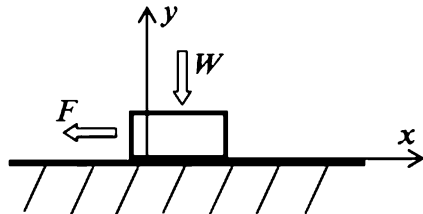
where μ is the coefficient of friction, which is independent of load, sliding velocity, and the nominal area of contact. Unlike many other linear empirical laws, the Coulomb law cannot be directly deduced from the linear equations of the nonequilibrium thermodynamics, such as (2.4). Indeed, in the case of dry or lubricated friction, the sliding velocity is the thermodynamic flow, $V = J$, which, in accordance with (2.7) should be proportional to the friction force $F = Y$ (as it is the case for the viscous friction), so that the energy dissipation rate is given by the product of the thermodynamic flow and force

$$\dot{\Psi} = JY = VF.\tag{2.11}$$

However, the Coulomb friction force is independent of sliding velocity.

We discuss in the ensuing chapters how to overcome this formal difficulty. In particular, we consider the normal degree of freedom y , in addition to the sliding coordinate x (Fig. 2.2). Introducing the normal degree of freedom is a standard procedure in the study of dynamic friction, where normal vibrations are often coupled with in-plane vibrations. We further define the generalized flows as $J_1 = \dot{x}$, $J_2 = \dot{y}$ and forces as $Y_1 = F$, $Y_2 = W$ (Nosonovsky 2009).

Fig. 2.2 Friction and the normal degree of freedom. The introduction of the normal degree of freedom, y , makes it possible to consider the Coulomb friction as a limiting case of the viscous friction and to include it into the linear Onsager scheme



The thermodynamic equations of motion (2.4) immediately yield the law of viscous friction in the form of

$$\begin{pmatrix} \dot{x} \\ \dot{y} \end{pmatrix} = \begin{bmatrix} L_{11} & L_{12} \\ L_{21} & L_{22} \end{bmatrix} \begin{pmatrix} F \\ W \end{pmatrix}. \quad (2.12)$$

Note that (2.12) is valid, in a general case, for the bulk of 3D deformable medium, and not necessarily for the interface between two solids.

The interface between sliding bodies has highly anisotropic properties, because a small force in the direction of the interface causes large displacements, whereas a small force in the normal direction causes only small displacements. To compensate for this anisotropy, we substitute coordinates using a small parameter ε as $(x, y) \rightarrow (\varepsilon x, y)$. The force–displacement relationships are now given by

$$\begin{pmatrix} \dot{x} \\ \dot{y} \end{pmatrix} = \begin{bmatrix} L_{11}/\varepsilon & L_{12}/\varepsilon \\ L_{21} & L_{22} \end{bmatrix} \begin{pmatrix} F \\ W \end{pmatrix}. \quad (2.13)$$

In the limit of $\varepsilon \rightarrow 0$, (2.13) yields

$$\begin{aligned} F &= -\frac{L_{12}}{L_{11}}W, \\ \dot{x} &= (L_{11}F + L_{12}W)/\varepsilon = 0/0, \\ \dot{y} &= \left(L_{22} - \frac{L_{12}L_{21}}{L_{11}} \right) W. \end{aligned} \quad (2.14)$$

According to (2.14), any velocity \dot{x} satisfies (2.13), provided $L_{11}F + L_{12}W = 0$, which is exactly the case of Coulomb friction if $\mu = -L_{12}/L_{11}$ (Nosonovsky 2009).

Thus, we showed that the Coulomb friction law (2.10) can be deduced from the thermodynamic equations of motion (2.4) provided two assumptions are made: (1) motion in the normal degree of freedom (y) is coupled with the tangential degree of freedom (x) and (2) the change of coordinates $(x, y) \rightarrow (\varepsilon x, y)$ is introduced and the limiting case of $\varepsilon \rightarrow 0$ is investigated. The normal degree of freedom was introduced into the analysis of dynamic friction since the pioneering works of Tolstoi (1967) who discovered the existence of natural normal microvibrations coupled with the tangential vibrations, which strongly affect the magnitude of the friction force as well as the stability of sliding. The introduction of a small parameter ε and an asymptotic decomposition is the standard way of the transition from 3D to a 2D problem

(e.g., from the bulk elastic 3D body to a thin elastic plate). The Coulomb friction is an interface (2D) phenomenon and it is natural to obtain its properties using an asymptotic limit of the 3D case (Nosonovsky 2009).

For a friction-induced deterioration, such as wear, the degradation force is proportional to the frictional dissipation (Fox-Rabinovich and Totten 2006; Bryant et al. 2008)

$$Y^{\text{deg}} = \alpha F \dot{x}, \quad (2.15)$$

where α is a parameter needed from dimensional considerations (note that for ξ to have the dimension of wear volume and for ξY^{deg} to have the dimension of energy, the dimension of L and α should be $\text{m}^5 \text{s}^{-1} \text{N}^{-1}$ and $\text{m}^{-3} \text{s}$). Taking $L\alpha = k/(\mu H)$ immediately yields the Archard's wear law, which relates the rate of wear volume \dot{v} to the normal load, sliding velocity material hardness, H , and the nondimensional wear coefficient k

$$\dot{\xi} = k \frac{F \dot{x}}{\mu H}. \quad (2.16)$$

2.2.4 Optimization of Healing

Suppose that the coefficients in the governing Eq. (2.7) depend upon a micro/nanostructure parameter of the material Ψ , such as the size distribution or the concentration of microparticles embedded in a composite material, $L = L(\Psi)$, $M = M(\Psi)$, $H = H(\Psi)$. The problem of optimum design of a self-healing system can be seen as finding an optimum value of Ψ for the minimization of the degradation parameter.

For any self-healing mechanism, the following scheme is suggested. First, micro/nanostructure parameters critical for the self-healing mechanism, as well as relevant degradation and healing parameters are identified. Then thermodynamic flows and forces are related to the microstructure. The obtained system of equations is dependent upon Ψ and should be optimized by Ψ for the minimization of degradation.

For metallic materials, there are three main self-healing mechanisms that are currently being investigated by different research groups: (1) precipitation in alloys to close voids and cracks, (2) material reinforcement with embedded SMA microwires, and (3) embedding liquid healing agent into a matrix by microballoon encapsulation. In the precipitation mechanism, voids serve as nucleation centers for the diffusion of the oversaturated solute in the alloy (Fig. 1.2b). The size of the voids is the degradation parameter ξ , and the concentration of diffused solute is the healing parameter ζ , while the kinetics of the diffusion of the solute into the void is governed by a kinetic equation [similar to (2.4)]. The microstructure parameter of relevance is the concentration of the solute.

For material reinforcement with SMA microwires, the closing of the crack is achieved by heating the sample (Fig. 1.2c). The SMAs are capable of the shape memory effect due to their ability for temperature- and stress-induced reversible martensite/austenite phase transition (Perkins 1981a, b). This transition is only dependent on temperature and stress, not time (as most phase changes are), as there is no diffusion involved. The temperature of the transition is different during heating and cooling due to hysteresis. The martensitic phase can also be generated by stressing the metal in the austenitic state, and this martensite phase is capable of large strains. When the stress is released, the reversed martensite/austenite transition does not occur if the temperature remains above the transition temperature during cooling. However, when the temperature is raised above the transition temperature during heating, the martensite transforms back to the austenite phase and resumes its original shape. While the deformation of a SMA looks similar to plastic deformation, it is actually a reversible deformation. However, deformation of SMA-reinforced metal, unlike pure SMA, is not necessarily reversible, as residual stresses remain to be overcome, which can prevent the complete reoccurrence of the austenite phase. For an SMA-reinforced metal, the cross-sectional concentration of microwires can be the structural parameter Ψ , the volume of voids is the degradation parameter ξ , and the strain in SMA is the healing parameter ζ .

Encapsulation of a healing agent is used for crack damage repair. When the crack propagates, the capsule ruptures and liquid adhesive is released that can heal the crack (Fig. 1.2a). This method is especially successful with polymeric materials. Crack propagation is an irreversible process, because when intermolecular bonds are broken, the energy γ is released irreversibly, and a certain amount of entropy is produced. When a capsule ruptures and its content is released, the configurational entropy grows because mixing occurs. The macroscale entropy is reduced at the expense of the microscale entropy. For this mechanism, the total area of the cracks can be the degradation parameter ξ , the amount of released healing agent is the healing parameter ζ , and the concentration of microcapsules or microtubes is the structural parameter Ψ .

Self-healing mechanisms in metals are summarized in Table 2.1. We use the classification suggested by Van Der Zwaag (2007) and Manuel (2009). The table shows typical materials for the matrix and reinforcement, parameters that characterize microstructure, degradation, healing, characteristic length scales for the degradation and healing mechanisms, the type of phase transition involved in the healing, and what property is improved in the self-healing alloy. The nature of the healing force and details of healing mechanisms are discussed in the consequent section.

2.3 Self-Healing Metallic Systems

In this section, we review the three mechanisms of self-healing that are used for metallic materials, paying attention to thermodynamic flows and forces that act during healing. As described in the preceding section, self-healing is

Table 2.1 Self-healing mechanisms in metals

Mechanism	Precipitation	SMA reinforcement	Healing agent encapsulation
Type (according to Van Der Zwaag 2009)	Damage prevention	Damage management	
Type (according to Manuel 2009)	Solid-state	Solid-state (possibly also liquid assisted)	Liquid-assisted
Matrix material	Al–Cu, Fe–B–Ce, Fe–B–N, etc.	Sn–Bi, Mg–Zn	Al
Reinforcement materials	–	NiTi	Sn–Pb
Microstructure parameter, Ψ	Solute fraction	Concentration of microwires	Concentration of microcapsules or low-melting point alloy
Degradation measure, ξ	Volume of voids	Volume of voids	Volume of voids
Healing measure, ζ	Amount of precipitated solute	SMA strain	Amount of released healing agent
Characteristic length of degradation	Void size (microscale)	Void/crack size (macroscale)	Void/crack size (macroscale)
Characteristic length of the healing mechanism	Atomic scale (atomic diffusion)	Microwires diameter (macro or microscale)	Microcapsule size (microscale)
Phase transition involved	Solute precipitation	Martensite/austenite	Solidification of the solder
Healing temperature	Ambient	Martensite/austenite transition	Melting of the low-melting point alloy
Property improved	Creep resistance	Restored strength and toughness	Restored strength and fracture toughness

achieved by bringing the system out of thermodynamic equilibrium and coupling the restoring force with the degradation parameter.

2.3.1 Damage Prevention by Precipitation in Under-Aged Alloys

It is difficult to facilitate healing in metallic materials because atoms of metals have much lower diffusion rates compared to polymers, and they remain solid at higher temperatures. One of the techniques to provide the atomic transport of matter to voids and defects in metals is to use a supersaturated solid solution in alloys, which has a decreasing solid solubility of solute elements with decreasing

temperature (e.g., Al–Cu). Such an alloy, when quenched from high temperature, becomes supersaturated, or metastable. A typical phase diagram of an alloy capable of precipitation strengthening is presented in Fig. 2.3a (Lumley 2007). Solution treatment is conducted within a single-phase region of the phase diagram before quenching. After the heat treatment, the alloy is heated again into the $\alpha + \gamma$ phase region (γ is an intermetallic phase). However, in order to facilitate precipitation of the solute, heterogeneous nucleation sites are needed. Sites with high surface energy, such as voids, defects, grain boundaries, and free surfaces become nucleation sites and therefore an atomic flux J^{diff} due to diffusion given by Fick's law

$$\begin{aligned} J^{\text{diff}} &= -D\nabla\zeta, \\ D &= D_0 \exp(-Q/RT), \end{aligned} \quad (2.17)$$

where $\nabla\zeta$ is the spatial gradient of the concentration, D is the diffusion coefficient, D_0 is the frequency factor, Q is the activation energy, $R = 8.31 \text{ J K mol}^{-1}$ is the gas constant, and T is the absolute temperature (Lumley 2007). Figure 2.3b presents a micrograph of dynamic precipitation of an under-aged Al–Cu–Mg–Ag alloy following 500 h creep at 300 MPa and 150°C (Lumley 2007). Bands of dynamically precipitated particles were formed and associated with dislocations (marked by arrows) – examples of the dynamically precipitated phase are marked “A.” Lumley (2007) investigated creep behavior of the 2024 Al alloy. Creep curves for the under aged, heat treated, and artificially aged T6 alloys are shown in Fig. 2.3c (based on Lumley 2007).

The method known as age hardening or precipitation hardening is routinely used in metallurgy to increase the yield strength of an alloy by producing fine particles of an impurity phase, which impede the movement of dislocations, or defects in a crystal's lattice. Depending on the time of age hardening, an alloy can be under-aged (with many small size of precipitation particles) or over-aged (with few large particles).

An under-aged alloy can be used to provide a self-healing mechanism. When an age-hardened aluminum alloy is solution treated at high temperatures, and quenched and annealed for a relatively short period at elevated temperatures, an under-aged microstructure is produced that still retains a substantial amount of solute in the solid solution. These solute atoms can diffuse into the open-volume defects created by plastic deformation at elevated temperatures. As the degradation ξ grows, the high-energy void sites emerge, and the concentration gradient $Y^{\text{heal}} = -\nabla\zeta$ grows, resulting in the flow of the solute, which serves as the healing agent. The solute fills the void, effectively closing it, thus decreasing the degradation – in other words; the concentration gradient is coupled with the degradation flow $\dot{\xi} = MY^{\text{heal}}$. Therefore, the (2.7) is given by

$$\begin{aligned} \dot{\xi} &= L(\Psi, T)Y^{\text{deg}} - M(\Psi, T)\nabla\zeta, \\ \dot{\xi} &= M(\Psi, T)Y^{\text{deg}} - D(\Psi, T)\nabla\zeta, \end{aligned} \quad (2.18)$$

where Ψ is a microstructure parameter, i.e., the percentage concentration of the solute. The problem of microstructure optimization is then formulated as finding the optimum value of Ψ that provides the most efficient healing for the typical values of the degradation forces. The diffusion coefficient can have a complex dependence on Ψ and T , and so is the coefficient M , so the task of finding the optimum Ψ to minimize fatigue remains to be solved.

Self-healing alloys that employ the precipitation of the solute serving as a healing agent were successfully developed on the basis of aluminum and steel. In these alloys, the main parameter that characterizes the efficiency of healing is the creep life of the alloy. The precipitation effectively prevents creep and damage. It is difficult to observe the precipitation events directly; however, positron annihilation spectroscopy (PAS) allows quantitative measurement of solute atom/vacancy interaction and it is especially powerful when used in conjunction with a 3D atom probe field ion microscopy (Lumley 2007). PAS involves the trapping of positrons in open volume defects such as voids or vacancies, followed by annihilation with an electron into two 511 keV gamma quanta after a time period (lifetime), which is measured and is typically between 100 and 500 ps.

Van Der Zwaag and co-workers (Hautakangas et al. 2007a, b, 2008) investigated creep in under-aged Al–Cu–Mg–Ag alloys and found that dynamic precipitation, in which the movement of dislocations under load promotes the nucleation of precipitates at the defect sites, is a strong self-healing mechanism in these alloys. The initial concentration of open volume defects is larger in the under aged and deformed material than in the un-deformed material. However, after aging at room temperature, rapid diffusion of the retained copper solute atoms to the open volume defects causes the concentration of open volume defects to approach their concentration in the un-deformed material. The under-aged material is thus effectively “healed” through the room temperature aging process, due to the annihilation of the open volume defects, which can coalesce to form cracks. This is not observed in the fully aged material. This study of the effect of aging on a commercial Al2024 alloy was performed in order to investigate self-healing in metal alloys. The alloy was preheated, treated, and aged at room temperature after solutionization. Positron annihilation was performed to measure the average positron lifetime (on the order of hundreds of ps) in vacancies, and it was observed that this value has decreased. The decay of the positron lifetime is related to the dispersion of vacancy defects during the aging process where the aluminum alloy exhibited some evidence of self-healing in the process of manufacturing. Although this under aging treatment is not what would be conventionally considered a self-healing process, the authors chose to view this prevention of void coalescence as a de facto self-healing mechanism. In such a case, the self-healing is considered to be an improvement in protecting the material against any damage.

Lumley et al. (2002, 2003) and co-workers (Buha et al. 2007; Lumley and Schaffer 2006) investigated the “secondary precipitation” in an Al–Cu alloy, i.e., the process where secondary aging occurring at a low temperature ($T = 65^\circ\text{C}$) resulted in much finer precipitates than the initial aging at a higher temperature ($T = 220^\circ\text{C}$). They also investigated dynamic precipitation in Al–Cu–Mg–Ag

alloys that occurs in response to the generation of moving dislocations when material is under load, and found that it has potential for self-healing during fatigue and creep (Lumley et al. 2002; Hautakangas et al. 2006; 2007a, b, 2008; Zhu et al. 2000).

Laha et al. (2005, 2007a, b) studied precipitation in an austenitic stainless steel modified with boron and cerium. An improvement of creep strength coupled with creep ductility of the steel was observed and attributed to the precipitation. Similar results were observed with the steel matrix supersaturated with N, Cu, B, or Ce atoms (Shinya et al. 2006; He et al. 2009).

2.3.2 Composite Materials Reinforced with Shape-Memory Alloys

A different approach to self-healing was used by Manuel, Olson, and co-workers (2007). Their approach involves embedding SMA reinforcement microwires into the metal matrix. The SMA transforms from the martensite to the austenite phase upon heating, and back to the martensite phase upon cooling. In the martensite state, the SMA can be easily deformed. However, unlike in the case of plastic deformation that is caused by irreversible dislocation or atomic plane slip, the martensite deformation is reversible. This is because the martensite material responds to stress by “twinning,” or changing the orientation of its crystal structure (Brinson 1993; Burton et al. 2006). In the martensite state, there are many variants of orientation of the crystal; however, they all correspond to only one possible austenite orientation. Therefore, when the martensite \rightarrow austenite transition occurs during heating, the crystal is forced to return to its original (nondeformed) shape. The crystal keeps this nondeformed shape after the austenite \rightarrow martensite transition upon cooling (Fig. 2.4). Note that during the twinning deformation of the martensite crystal, the energy is dissipated and not accumulated in the material; however, after the transition to the austenite state the energy depends on the strain.

Manuel and Olson (2007) synthesized a self-healing composite using a Sn–21Bi (wt%) alloy reinforced with 1% equiatomic NiTi SMA wires. The diameter of the wire was 190.5 μm . The temperature of transition for the wire was increased to optimize the composite self-healing by aging at 500°C. The wires were coated with gold to improve their wettability with the matrix. The reinforced alloy displayed a 73% increase in uniform ductility, compared with an unreinforced matrix. After a complete matrix fracture, the alloy was healed at 169°C for 24 h (resulting in the austenite transition of the SMA and partial melting of the matrix) and demonstrated a 95% tensile strength recovery (Fig. 2.5). The healing temperature was selected to assure that between 15 and 20% of the matrix around the crack gets liquefied to provide good welding of the crack as a result of compressive forces generated by the phase transition of the SMA. Manuel also investigated the optimum size and volume fraction of the reinforcing SMA microwires (Fig. 2.6) Manuel (2009).

Olson et al. obtained similar results with Mg-based alloys reinforced with thermally stable, precipitation-strengthened, multicomponent SMA combining

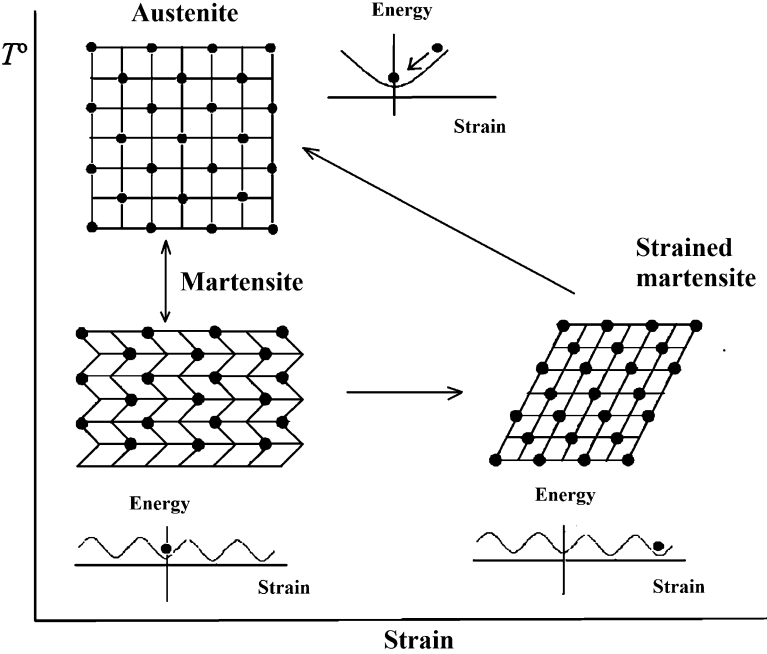


Fig. 2.4 Energy transitions in a shape-memory alloy. Dissipation occurs during the deformation in the martensite state. However, the strain energy restores when the martensite–austenite phase transition occurs

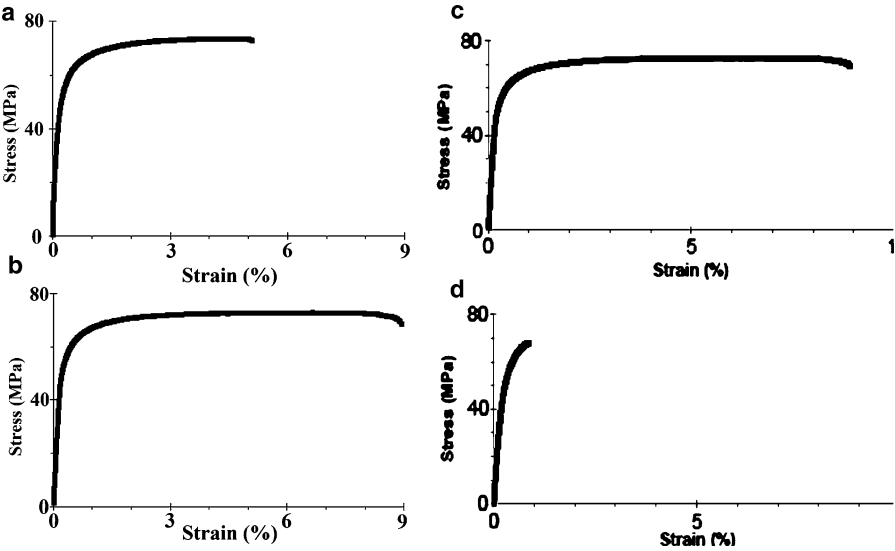
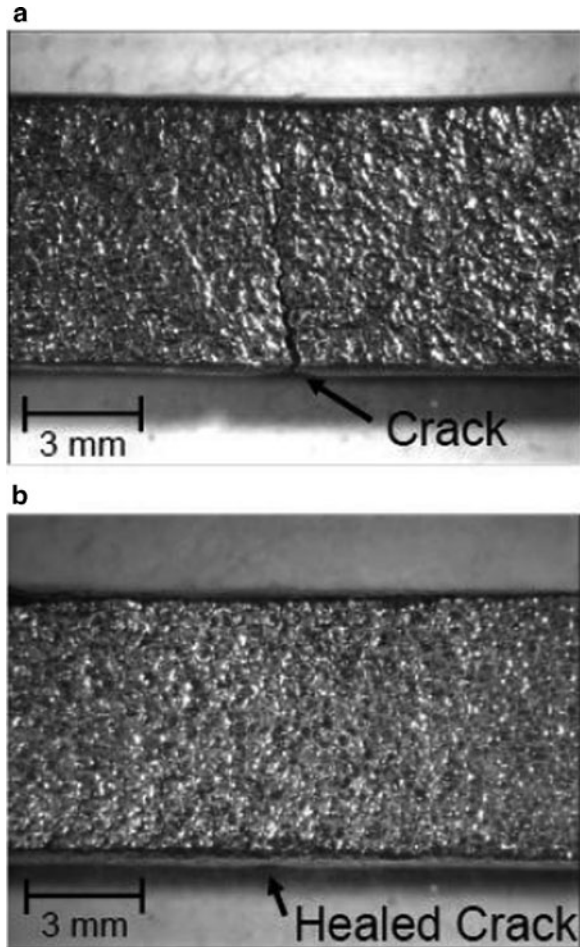


Fig. 2.5 Stress–strain diagram for heat-treated Sn – 13 at.% Bi proof-of-concept matrix and composite with 1% volume fraction of SMA wires (a) before and (b) after healing (adapted from Manuel 2009)

Fig. 2.6 Optical micrographs of a fractured Sn – 13 at.% Bi proof-of-concept composite (a) before and (b) after healing. It is evident that the composite was able to heal a macroscopic crack (Manuel 2009)



high-structural performance and processability (Fig. 2.7) Manuel (2009). The high-specific strength of Mg makes it an attractive option as a lightweight structural element; however, the crystal structure and microstructure of Mg causes low ductility and poor toughness. This low toughness limits the use of Mg in engineering structural applications. Nevertheless, Mg is considered a good candidate for the matrix in a self-healing alloy, provided self-healing will enhance toughness. A magnesium-based alloy was reinforced with TiNi SMA wire with a diameter of $190.5\text{ }\mu\text{m}$. Before casting, the nitinol wires were embedded in Pyrex and annealed at 500°C for 3 h. The objective of this heat treatment is to increase the temperature of the phase transition. The limitation with Mg-based alloys is that they do not “weld” to themselves, like the Sn–Bi alloy did in the proof of concept experiment (Fig. 2.8).

It is natural to take the volume of voids and crack openings as the degradation parameter ξ , and the strain of the SMA microwires as the healing parameter ζ , while the concentration of the microwires is the microstructure parameter, Ψ . When the

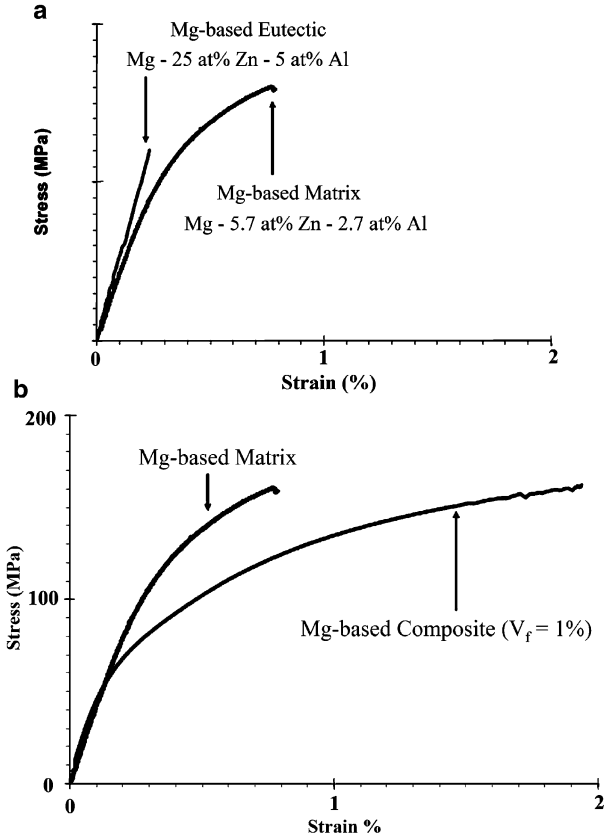


Fig. 2.7 Comparison of stress–strain curves for the heat-treated Mg-based eutectic and heat-treated Mg-based matrix alloys and Mg-based matrix and composite (1%) alloys (Manuel 2009)

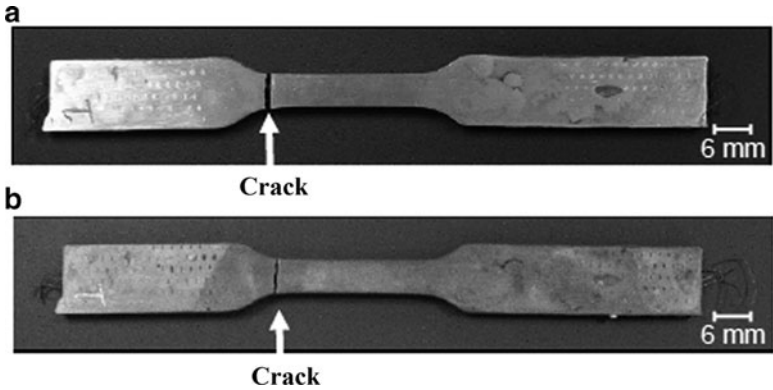


Fig. 2.8 Fractured Mg-based self-healing alloy composite (a) before and (b) after healing (Manuel 2009)

system is healed, it undergoes the martensite→austenite transition due to the elevated temperature. At this point the system is brought to a nonequilibrium state, with the amount of the excess energy dependent on ξ . We assume that the restoring thermodynamic force is approximately proportional to the strain $Y^{\text{heal}} \propto \zeta$, and that the strain rate is proportional to the restoring force. Since the healing is achieved by the transition to the austenite phase, we take this as the healing parameter, ζ , and the fraction of the austenite state in the SMA.

$$\begin{aligned}\dot{\xi} &= L(\Psi, T)Y^{\text{deg}} - M(\Psi, T)\xi, \\ \dot{\zeta} &= M(\Psi, T)Y^{\text{deg}} - H(\Psi, T)\zeta.\end{aligned}\tag{2.19}$$

The problem of microstructure optimization is now reduced to the mathematical problem of finding the optimum value of Ψ that provides the best healing at the needed temperatures and degradation force levels.

To take the degradation force into consideration, a particular mechanism of degradation should be included. For friction-induced degradation (e.g., wear) the description given by (2.14)–(2.16) should apply, whereas for crack propagation the equations of fracture mechanics should be used.

2.3.3 Composite Materials Reinforced with a Healing Agent

A self-healing composite can also be produced by incorporating a low-melting temperature alloy that serves as a healing agent in a high-melting temperature alloy which serves as a matrix, using the methodology of metal matrix composites (Rohatgi et al. 1979, 1986; Ghosh et al. 1984; Jha et al. 1989). Lucci et al. (2008a, b, c) studied a composite consisting of an Al alloy 206 matrix reinforced with hollow ceramic tubes whose hollow spaces were infiltrated with a lower melting point (Sn60Pb40) alloy (a solder). When the low-melting point alloy encapsulated in the hollow cavities of the tubes reached the healing temperature, it became completely molten, and due to capillary pressure and surface tension, it would under certain conditions, flow out of the ceramic tube and fill in the crack. As the temperature decreased, the low-melting point healing alloy solidified and sealed the crack. The flow of the low-melting point alloy, as a liquid “healing agent,” into the crack, and the sealing of the crack through solidification, can lead to the recovery of a high percentage of the original mechanical properties. A crucial property of this design is the bond between the Al matrix and the solder alloy solidified in the crack. If the bond between the solidified healing agent and the aluminum matrix is poor, the crack may continue to propagate through the aluminum matrix. An optimized model and design for this self healing material would be difficult to obtain using a trial and error approach, therefore, computational fluid analysis (CFD) could be used to obtain the parameters necessary to design the



Fig. 2.9 Front view of the self-healing composite (Nosonovsky et al. 2009)

self-healing composite (Lee et al. 2007; Xiao and Amano 2006; Chen et al. 2005; Kalra et al. 2003; Lucci et al. 2008a, b, c).

The tubes were aligned only in one direction; one purpose of using ceramic tubes is to reinforce the matrix. The tube dimensions diameters were 2.185 mm inside and 3.95 mm outside, while the length was 75 mm. A total of seven tubes were placed in a mold held by a wire mesh to prevent any misalignment during the casting. Aluminum alloy 206 was cast only slightly above the liquidus temperature for the alloy in a steel mold, which contained the alumina tubes. A relatively low pouring temperature was used to avoid precracking the alumina tubes. The mold containing the alumina tubes was preheated. A fully dense portion of the casting was used in subsequent self-healing experiments. Figure 2.9 shows the prototype of a self-healing composite. The hollow tubes were then filled with the solder alloy healing agent, by pressure infiltration. To demonstrate the concept of self-healing, the ends of the tubes were sealed with refractory cement to prevent leaking during the process of healing (Fig. 2.10).

A sample of the self-healing composite was produced and a 1-mm hole was drilled in the surface of the sample, piercing one of the tubes filled with the low-melting point alloy to simulate a crack running perpendicular to the tubes. The sample was then heated over the area of the low-melting point alloy above 300°C for 5 min and then cooled to room temperature. The solder flowed out of the microtubes and sealed the hole. A second sample was made from the matrix and a crack was created by drilling the matrix surface and cutting one of the tubes. The volume of the crack was 0.0948 cc. The external surface of the crack was then sealed with aluminum foil and both ends were refractory cemented. Gravity plays a very important role in the design of the process of self-healing; to understand this

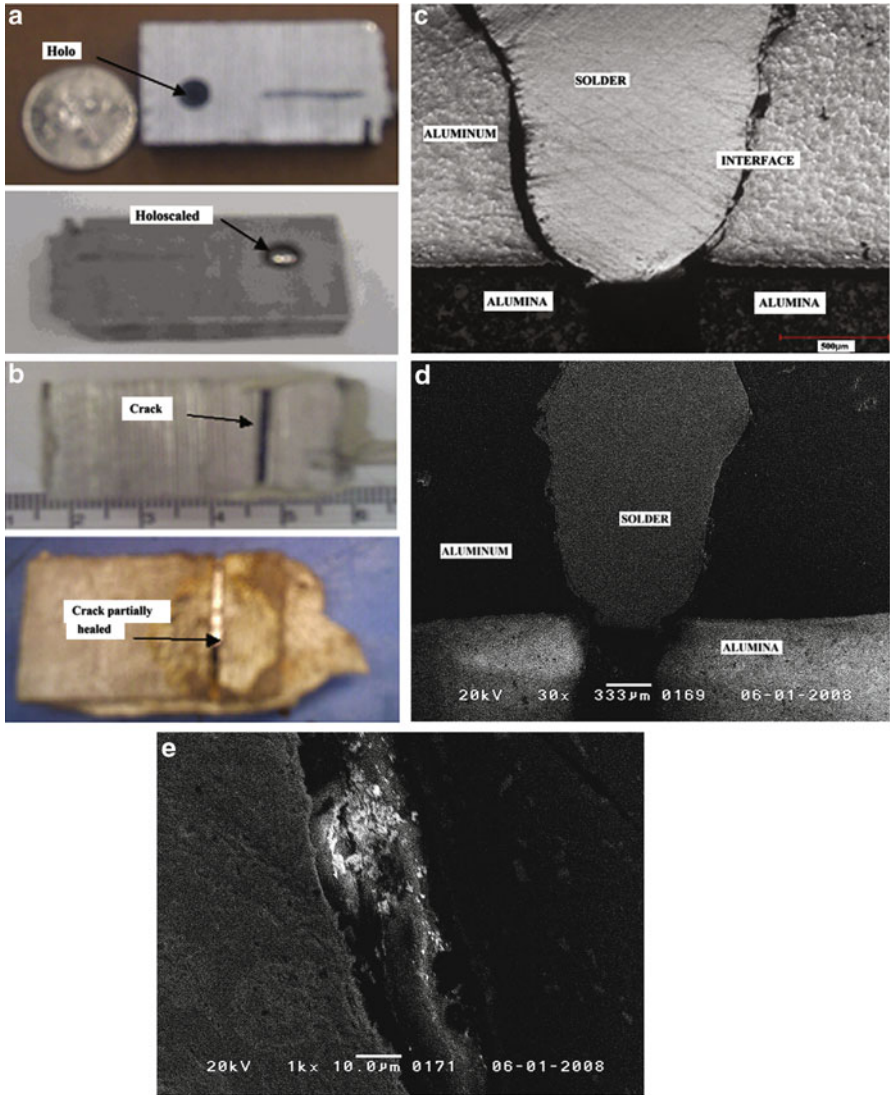


Fig. 2.10 (a) Self healing composite with hole (*upper*) and the sealed hole after heating (*lower*); (b) before and after healing the specimen; (c) the bond between Al206 and solder after healing; (d) microstructure of the healed composite (SEM); (e) interface between Al206 and solder after healing (SEM) (Lucci et al. 2008b)

effect the samples were placed crack face down on a plate, and then heated above the melting temperature of the solder. The composite was then cooled to ambient temperature. The healing process in this case involved sealing the damaged wall however, the damaged specimen was only partially healed by the solder (the result of this process is observed in Fig. 2.10a). One possible reason why the solder

did not fill the entire crack may be the low wettability between the matrix and solder surface, and the fluidity for infiltration into the entire length of the crack. Thus, the interface between the matrix and the self-healing molten solder and its wetting properties are crucial and require an in-depth investigation.

Figure 2.10b shows the microscopic structure of the sealed crack. The crack is only partially sealed and the bond between the aluminum and the solder has high interfacial porosity, thus the bond is likely not strong enough to stop the crack in the transversal direction of the matrix.

Figure 2.10c shows the scanning electron microscope (SEM) micrographs of the polished microstructure of the interface between a section of the “cracked” aluminum and the solder, as viewed with a Topcon SM300 SEM. Energy dispersive X-ray spectroscopy (EDS) point analysis was used to determine the elemental composition of the solder region versus the aluminum region and near the interface between the two.

The interfacial bonding between the solder within the crack and the walls of the crack is poor; the solidified solder is not in intimate contact with the aluminum matrix in the observed cross section. The porosity near the walls of the crack appears to have formed due to a lack of wetting and shrinkage as the solder solidified within the crack. No apparent reactions or bonding have occurred between the solder alloy (Sn–Pb) and the aluminum alloy (Al–Cu). Likewise there appears to be no reaction or bonding between the solder and the aluminum oxide tube. Therefore, further development in the synthesis of self-healing composites must focus on improving wetting and bonding between the healing agent (in this case the solder) and the walls of the crack in the aluminum matrix, which may even get oxidized if the crack is open to air. This is necessary to improve the properties of the healed composite (Fig. 2.10e).

Computational fluid dynamics (CFD) modeling was used to study the flow of liquids in and out of the reinforcements into cracks. The change of the phase occurring due to solidification was taken into account in the computational code. The wetting, capillarity, viscosity, and solidification will need to be tailored to achieve self-healing as a result of the flow of the low-melting point metal, its solidification in the crack, and its bonding with the crack surface. Modeling was done to select the optimum microstructure to get the most effective self-healing behavior. The simulation was done for different thicknesses of holes: 1 mm, 0.25 mm, and 10 μm with angles of 30°, 60°, and 90° relative to gravity to investigate the effect of capillarity. The simulation predicted the possibility of healing when the flow of healing liquid was toward the gravity force for a crack size between 10 μm and 1 mm. The CFD simulations conducted by Martinez Lucci (2011) showed a good agreement with the experiments.

The conclusion of this study was that wetting and capillary interactions between the molten solder and the crack/void cavity are crucial for healing. In this case, we can take the volume of voids and crack openings as the degradation parameter ξ , the amount of released solder as the healing parameter ζ , while the initial concentration of the solder as the microstructure parameter, Ψ . The diffusion of the solder into the cavity is governed by a diffusion-type equation or by a fluid flow equation,

while the healing force depends on both the amount of released solder and the volume of voids

$$\begin{aligned}\dot{\xi} &= L(\Psi, T)Y^{\text{deg}} - M(\Psi, T)Y^{\text{heal}}(\xi, \varsigma), \\ \dot{\varsigma} &= M(\Psi, T)Y^{\text{deg}} - D(\Psi, T)Y^{\text{heal}}(\xi, \varsigma).\end{aligned}\quad (2.20)$$

A quantitative analysis was suggested by Nosonovsky et al. (2009, 2010a), which found a reasonable qualitative agreement of the model with the experimental data. Again, the nature of voids and cracks was not the consideration; however it may, in principle, be included by using (2.14)–(2.16) for friction-induced degradation or similar equations for other types of degradation (e.g., fracture).

2.4 Future Approaches

In the preceding section, we described the methods that are currently used to implement self-healing in metals. These methods have a number of limitations. First, all of the methods require an input of external thermal energy. Whereas some Al alloys can age at room temperature, most of the precipitation events shown in the studies were at an elevated temperature. The SMA-reinforced and solder-in-tube/capsule composites also required elevated temperature for the phase transformation to occur to initiate healing.

Second, there is a limitation on the type of materials for which the self-healing mechanisms can be applied. Precipitation-induced healing requires that the solute remain in solution, so the method can only apply to select combinations of materials. The precipitation events will also occur over time without stress, and the formation of defects and the retained solute healing agent will be exhausted and not available for healing (Lumley et al. 2002). SMA-reinforced healing requires an alloy that can bond to itself, thus closing the crack. Otherwise additional measures (e.g., partial melting) are needed to provide the crack/void sealing. The use of an embedded healing agent does not by itself provide a mechanism to regain the volume. It is desirable to implement such a mechanism (e.g., a chemical reaction), because without it, regaining mechanical strength remains questionable. The conflicting requirements of self-healing and mechanical properties are to be balanced for an effective self-healing composite material.

Several other possible approaches have been suggested to improve self-healing in metals and to fix deficiencies in the current methods. One approach is to mimic the healing of skin, where cutting the skin triggers blood flow, coagulation and sealing of the cut due to the network of vessels and veins. The vascular network is a tree-like hierarchical structure that provides a uniform and continuous distribution of fluids throughout the material volume (Kim et al. 2006; Lee et al. 2008). Vascularization has been successfully used for polymeric composites and is expected to provide effective healing in metals as well (Therriault et al. 2003).

Material processing techniques which can incorporate a vascular network into the matrix are becoming available.

A self-healing method involving two concentric cylinders of conducting material filled with a liquid solution containing electromagnetic particles of polystyrene or silica was suggested. When damage occurs, voltage is applied between the inner pipe and outer pipe which results in the current density naturally increasing at the location of the damage. This increase in current density causes particle coagulation at the damage site, which is a way to heal the damage (Slowik 2009).

Brinker technology has developed a method to seal and locate the leakage in subsea and water pipelines. This technique is named Platelet Technology, and inspired by the method that the human body uses to seal wounds or scars on the skin. The particles are injected remotely into a pipeline, upstream of a damage site. They are carried with the flow in the pipeline and when the particles reach the leak, the fluid force exerts a pressure on the particles which holds them against the pipeline walls and seals the leak completely. In a water pipeline, the design of the particles must satisfy some requirements: the platelets must be neutrally buoyant, odorless, flavorless, nontoxic, and not promote the growth of microorganisms (Ryan 2007).

The incorporation of microballoons filled with a chemical that reacts with oxygen is another method. Thermite composites can be candidates for these materials. When the composite is damaged by a crack, the microballoons are broken as a result of the stress intensification due to the crack and the chemical will react with the oxygen in the air. This reaction increases the temperature around the crack surface to above the melting point of the metal, and the metal around the crack will melt and seal the crack. This method will only slightly deteriorate the mechanical properties with a crack closure; therefore the recovery of the mechanical properties of the composite will be high.

The incorporation of nanotubes filled with a low melting-point alloy into the metal matrix can constitute another approach to incorporate self-repair. The possibility of incorporating nanotubes into metals has been shown in the literature (Sen et al. 1997; Liu et al. 2004; Belko et al. 2007). This method will involve infiltrating a low-melting point alloy into the hollow cavities of nanotubes which will be embedded into the metal matrix. Nanotubes could be able to provide a more uniform distribution of the healing agent in the volume of the material compared to microtubes. The improvement of the mechanical properties of the metal matrix as a result of the incorporation of nanotubes is one of the advantages of using this method, compared to an incorporation of micro and macrotubes which may decrease certain mechanical properties of the matrix. Another advantage may be the possible closure of nanosize cracks.

Another more exotic approach, which has been used for polymers as well as concrete, is to incorporate bacteria into a metal matrix, so that when the composite is damaged, the bacteria will work to close a crack or repair the damage (Jonkers 2007; Jonkers and Schlangen 2009). The principle mechanism of bacterial crack healing is that the spore-forming bacteria themselves act largely as the catalyst and can transform a precursor compound into a suitable filler material.

However, it remains to be seen if bacteria-based self-healing is feasible in metallic materials, due to the high temperatures required for processing.

The field of coatings that are used to prevent or heal damage on metallic surfaces should be mentioned. Self-healing through the high temperature oxidation of Zr, Si, or Al in coating materials can be classified as a method of self-healing in metallic materials. Vitreous enamel coating for metal substrates have also been suggested in the literature (Zucchelli et al. 2009). Coatings are of special interest because, as discussed above, most degradation tends to start or occur at the interface. Sloof (2007, 2009) studied self-healing mechanisms in coatings at high temperatures. It was found that damage can be repaired by selective oxidation of the metallic alloy, if the component operates in an oxidizing environment, the alloy contains sufficient healing agent (i.e., the selectively oxidized element) and the diffusion of this element in the alloy is fast enough.

The design and synthesis of self-healing materials remain, to a large extent, as an experimental science, or even an art. In most cases, a trial-and-error approach is used to select appropriate material compositions and concentrations of components. In this situation, it may be promising to try to develop a more solid theoretical ground for self-healing. As we have shown in the above sections, most types of self-healing mechanisms are well described in terms of the nonequilibrium thermodynamics. It is expected that in principle it is possible to optimize the microstructure design using the nonequilibrium thermodynamic approach. However, to show experimental validation of these approaches remains an important future task.

2.5 Summary

Self-healing inorganic materials is a relatively new area in materials science and engineering. Inspired by living nature and modern technological opportunities, scientists are trying to implement in engineered materials, the ability for self-repair, which previously was found only in living nature. The ability to self-heal is related to the general ability of many systems for self-organization and can be described in terms of nonequilibrium thermodynamics. To provide self-organization, usually a special multiscale structure of a material is needed that allows for the maintenance of the macroscale entropy and thus maintains orderliness at the expense of the micro/nanoscale/atomic scale entropy growth.

We reviewed three main approaches to self-healing in metals and found that all of them involve multiscale organization with healing mechanisms acting at a lower scale level than the degradation mechanisms. The healing kinetics in each mechanism is described with similar nonequilibrium thermodynamics equations that relate the healing and degradation parameters and the generalized forces. The healing is achieved by coupling the degradation parameter to the generalized healing force. The healing force is induced by shifting the system away from thermodynamic equilibrium. The degradation force depends on the nature of the system and can be induced, for example, by friction.

Self-healing metals such as aluminum are potentially extremely beneficial for a wide range of industrial applications. A number of specific approaches to create self-healing metallic materials have been suggested. A number of specific obstacles should be dealt with – in particular, wetting and sufficient capillary pressure should be provided for a liquid solder to be able to infiltrate into the crack cavities. It should be kept in mind also that a self-healing requirement is often in conflict with mechanical properties (such as strength) and self-healing often cannot provide a complete recovery of undamaged material. A number of potentially useful approaches to improve performance of self-healing metallic materials have been suggested in the field. We expect that combining the fundamental thermodynamic approach of self-organization with the new advances in the synthesis of self-healing components will lead to more systematic and proactive ways of synthesizing these materials.



<http://www.springer.com/978-1-4614-0925-0>

Biomimetics in Materials Science
Self-Healing, Self-Lubricating, and Self-Cleaning
Materials

Nosonovsky, M.; Rohatgi, P.K.

2012, XXVI, 418 p., Hardcover

ISBN: 978-1-4614-0925-0